HHS Public Access

Author manuscript

Cell Rep. Author manuscript; available in PMC 2020 January 10.

Published in final edited form as:

Cell Rep. 2019 December 24; 29(13): 4460–4470.e8. doi:10.1016/j.celrep.2019.11.084.

Identification of Antibodies Targeting the H3N2 Hemagglutinin Receptor Binding Site following Vaccination of Humans

Seth J. Zost[1], **Juhye Lee**[2,3], **Megan E. Gumina**[1], **Kaela Parkhouse**[1], **Carole Henry**[4], **Nicholas C. Wu**[5], **Chang-Chun D. Lee**[5], **Ian A. Wilson**[5,6], **Patrick C. Wilson**[4], **Jesse D. Bloom**[2,3,7], **Scott E. Hensley**[1,8,*]

[1]Department of Microbiology, Perelman School of Medicine, University of Pennsylvania, Philadelphia, PA 19104, USA

[2]Department of Basic Sciences and Computational Biology Program, Fred Hutchinson Cancer Research Center, Seattle, WA 98109, USA

[3]Department of Genome Sciences, University of Washington, Seattle, WA 98109, USA

[4]Department of Medicine, Section of Rheumatology, the Knapp Center for Lupus and Immunology, University of Chicago, Chicago, IL 60637, USA

[5]Department of Integrative Structural and Computational Biology, The Scripps Research Institute, La Jolla, CA 92037, USA

[6]The Skaggs Institute for Chemical Biology, The Scripps Research Institute, La Jolla, CA 92037, USA

[7]Howard Hughes Medical Institute, Seattle, WA 98109, USA

[8]Lead Contact

SUMMARY

Antibodies targeting the receptor binding site (RBS) of the influenza virus hemagglutinin (HA) protein are usually not broadly reactive because their footprints are typically large and extend to nearby variable HA residues. Here, we identify several human H3N2 HA RBS-targeting monoclonal antibodies (mAbs) that are sensitive to substitutions in conventional antigenic sites and are therefore not broadly reactive. However, we also identify an H3N2 HA RBS-targeting mAb that is exceptionally broadly reactive despite being sensitive to substitutions in residues outside of the RBS. We show that similar antibodies are present at measurable levels in the sera of

*Correspondence: hensley@pennmedicine.upenn.edu.

AUTHOR CONTRIBUTIONS

S.J.Z., J.L., M.E.G., K.P., N.C.W., and C.-C.D.L. completed experiments and analyzed data. C.H. and P.C.W. provided plasmids that express heavy and light chains of each mAb in this study. J.D.B. supervised mutational scanning experiments. I.A.W. supervised Fab experiments. S.E.H. conceived the project, supervised the project, and analyzed data. S.J.Z. and S.E.H. wrote the manuscript with input from all authors.

DECLARATION OF INTERESTS

S.E.H. reports receiving consulting fees from Sanofi Pasteur, Lumen, Novavax, and Merck.

SUPPLEMENTAL INFORMATION

Supplemental Information can be found online at https://doi.org/10.1016/j.celrep.2019.11.084.

some individuals but that they are inefficiently elicited by conventional vaccines. Our data indicate that HA RBS-targeting antibodies can be effective against variable viral strains even when they are somewhat sensitive to substitutions in HA residues adjacent to the RBS.

Graphical Abstract

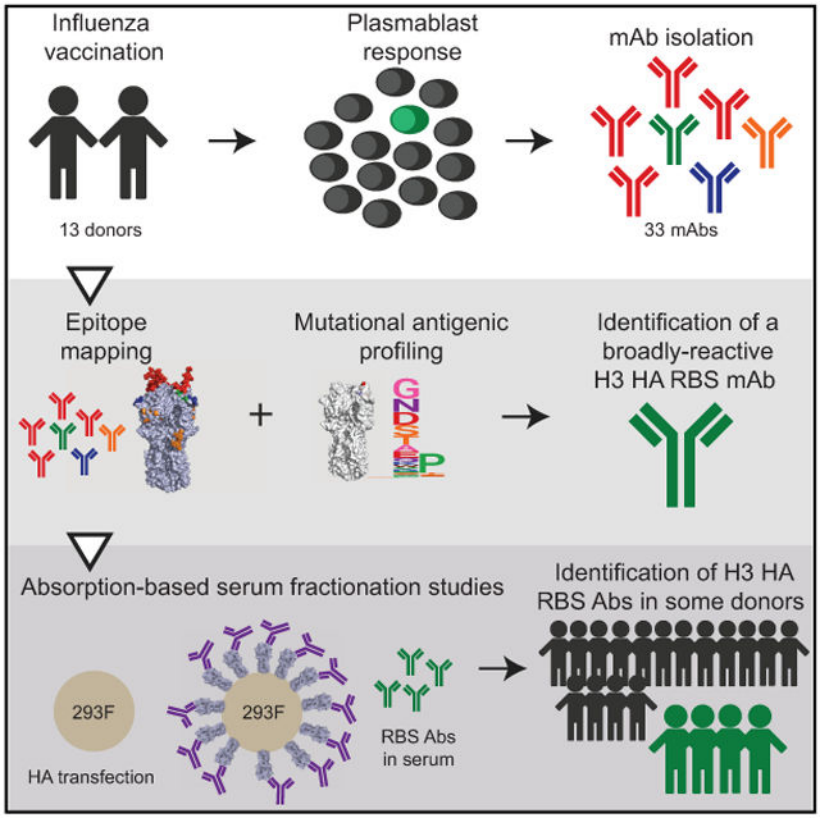

In Brief

Zost et al. show that most antibodies targeting the RBS of the H3N2 HAs are not broadly reactive. They identify one broadly reactive H3 HA RBS antibody that is tolerant of substitutions in adjacent antigenic sites but show that these types of antibodies are not efficiently elicited by vaccination.

INTRODUCTION

Influenza viruses continuously infect humans, in large part due to their ability to rapidly escape human immunity (Yewdell, 2011). Most neutralizing antibodies against influenza viruses target the globular head domain of hemagglutinin (HA) proteins and inhibit viral replication by blocking viral attachment. These types of antibodies often become ineffective after viruses acquire substitutions in epitopes within the HA globular head through a process called antigenic drift. As a result, seasonal influenza virus infections or vaccinations typically provide limited protection against antigenically drifted strains. New “universal” vaccine antigens are currently being developed to elicit broadly reactive antibodies against

conserved epitopes in the HA receptor binding site (RBS) (Giles and Ross, 2011; Kanekiyo et al., 2019) as well as the HA stalk region (Impagliazzo et al., 2015; Krammer et al., 2013; Yassine et al., 2015).

New universal vaccines that elicit antibodies against conserved epitopes in the HA RBS are attractive since antibodies against this region of HA directly block viral attachment and are highly neutralizing (Krause et al., 2011; Whittle et al., 2011). However, it is difficult to design vaccine antigens to elicit broadly neutralizing HA RBS-reactive antibodies because the surface area of most antibody footprints is larger than the narrow conserved RBS (Knossow and Skehel, 2006). The HA RBS is approximately 800 $Å^2$ (Weis et al., 1988), whereas most antibody footprints are 1,200–1,500 $Å^2$ (Amit et al., 1986).

Several broadly neutralizing antibodies that target conserved residues in the HA RBS have been identified (Ekiert et al., 2012; Krause et al., 2011; Lee et al., 2012, 2014; McCarthy et al., 2018; Schmidt et al., 2015b; Tsibane et al., 2012; Whittle et al., 2011; Winarski et al., 2015; Xu et al., 2013). These antibodies can arise from a number of V_H gene segments (McCarthy et al., 2018; Schmidt et al., 2015b). Most of these HA RBS-targeting antibodies bind through molecular mimicry, imitating the HA cellular receptor, sialic acid. Some of these broadly reactive antibodies make contact with conserved RBS residues through a shared dipeptide motif (Krause et al., 2011; Lee et al., 2014; Schmidt et al., 2015b; Whittle et al., 2011), while other antibodies insert a hydrophobic residue into the RBS (Lee et al., 2014; Xu et al., 2013). Most broadly reactive HA RBS-targeting antibodies have long heavy-chain complementarity determining regions (HCDRs) that allow the sialic acid-mimic motif of the antibody to be guided into the conserved RBS while minimizing contacts to variable residues on the rim of the RBS (Ekiert et al., 2012; Lee et al., 2014; Whittle et al., 2011; Xu et al., 2013).

Here, we delineated the binding and neutralization characteristics of a large panel of anti-H3 human monoclonal antibodies (mAbs) that were isolated following seasonal influenza vaccination. We found that a large proportion (>25%) of these mAbs targeted epitopes in the HA RBS. While most of these HA RBS-targeting mAbs were sensitive to substitutions in adjacent antigenic sites and were not broadly reactive, we identified one mAb that maintained broad reactivity despite being moderately sensitive to substitutions at residues inside and outside of the RBS. We completed a series of experiments to further characterize this mAb and determined that some individuals have high levels of similar antibodies in polyclonal sera.

RESULTS

Most Vaccine-Elicited Human H3 mAbs Target Epitopes in the HA Globular Head Domain

We characterized 33 anti-H3 human mAbs that were isolated from 13 individuals vaccinated with a 2010–2011 or 2011–2012 trivalent seasonal influenza vaccine (Table S1). First, we completed hemagglutination-inhibition (HAI) and micro-neutralization (MN) assays with the H3N2 component of the vaccines, A/Victoria/210/2009, to determine if the mAbs prevent receptor binding and/or block virus infection *in vitro*. Twenty six out of 33 mAbs inhibited hemagglutination of the vaccine strain (Figure 1A), indicating that they likely

targeted epitopes in the HA globular head domain. All HAI^+ mAbs also neutralized the A/Victoria/210/2009 strain *in vitro* (Figure 1B). We identified 7 HAI^- mAbs (Figure 1A), and we found that two of these mAbs neutralized virus *in vitro*, while the remaining five were non-neutralizing (Figure 1B). The two HAI^- neutralizing mAbs inhibited binding of the HA stalk-reactive F49 mAb in competition assays (Figure S1), suggesting that these mAbs targeted epitopes in lower regions of HA. These data are consistent with previous studies (Angeletti and Yewdell, 2018) that suggest that the majority of antibodies elicited by seasonal influenza vaccines target neutralizing epitopes on the HA globular head.

Most Vaccine-Elicited Human H3 mAbs Target HA Antigenic Site B

We then measured binding of each mAb to a panel of A/Victoria/210/2009 HAs that had different amino acid substitutions. For this, we created virus-like particles (VLPs) with A/Victoria/210/2009 HAs with substitutions in classic antigenic sites (Koel et al., 2013; Wiley et al., 1981) and antigenic sites that have recently changed in naturally circulating human viral strains (Hadfield et al., 2018). Most of the substitutions in our panel were located in the 140 loop of antigenic site A as well as the 150 loop and 190 helix of antigenic site B near the HA RBS, but we also included several substitutions in the lower part of the HA head (Figure 2A). We also included HAs with substitutions in conserved residues within the RBS (Figure 2B), so that we could identify HA RBS-targeting mAbs. In total, we tested binding of all 33 mAbs using a panel of VLPs that expressed the wild-type (WT) and 24 different mutant forms of A/Victoria/210/2009 HAs in ELISAs (Figure 2C).

The majority (73%) of HAI^+ mAbs in our panel were sensitive to substitutions in HA antigenic site B. Substitutions at residues 157, 159, and 160 of HA antigenic site B abrogated the binding of ~61% of HAI^+ mAbs, whereas substitutions at other antigenic site B residues (155, 156, 189, 192, 193) affected the binding of fewer mAbs. We identified a few mAbs that were sensitive to substitutions in antigenic site A or epitopes lower on HA that were further from the RBS. Only three mAbs in our panel were sensitive to substitutions in antigenic site A, and 7 mAbs were sensitive to substitutions in residues lower on HA. These data suggest that antigenic site B is the major target of human neutralizing HA antibodies to recent H3N2 strains and demonstrate that single substitutions near the RBS can abrogate the binding of most human mAbs.

While our data indicating that most of the mAbs in our panel are HA site B specific are consistent with previous studies (Chambers et al., 2015; Popova et al., 2012; Zost et al., 2017), we were surprised to find that ~1/3 of our HAI^+ mAbs were sensitive to substitutions in conserved positions in the HA RBS (Figure 2C). Most of the mAbs in our panel that were sensitive to RBS substitutions were also sensitive to site B substitutions (Figure 2C). However, several mAbs that targeted the HA RBS were only moderately affected by site B substitutions. For example, the 019-10117-3C06 mAb, which was moderately sensitive to RBS and site B substitutions, maintained partial binding to all of the mutant HAs that we tested. These data reveal that seasonal influenza vaccines elicit robust antibody responses targeting conserved residues within the HA RBS and that at least some of these antibodies can maintain partial binding to HAs that have substitutions in conventional antigenic sites adjacent to the RBS.

Identification of an HA RBS Targeting mAb with Exceptional Breadth

We measured binding of each mAb to HAs from H3N2 viruses isolated before and after the 2010–2012 seasons. As expected, most HAI^- mAbs bound broadly to H3 HAs isolated from 1968–2014 and two HAI^- mAbs bound to both H3s and H1 HAs (Figure 3). In contrast, the majority of HAI^+ mAbs bound to a narrow range of HAs from viruses that circulated from 2005–2012 (Figure 3). Most HAI^+ mAbs failed to recognize an HA from a recent 2014 clade 3C.2a H3N2 strain (Chambers et al., 2015; Zost et al., 2017) that has a more antigenically evolved HA antigenic site B (Figure 3). Interestingly, two HAI^+ mAbs (019-10117-3C06 and 028-10134-4F03) had exceptionally broad reactivity, binding to every H3 HA in our panel. One of these mAbs (028-10134-4F03) was sensitive to substitutions in residues 121 and 150 (Figure 2B) in the mid region of the HA head (Figure 2A). The second broadly reactive HAI^+ mAb (019-10117-3C06) is particularly interesting because it is one of the HA RBS-targeting mAbs that we determined to be only moderately sensitive to substitutions in classic antigenic site B (Figure 2B). Despite having moderate reductions in binding to HAs with antigenic site B substitutions and RBS substitutions, the 019-10117-3C06 mAb partially bound to every H3 HA in our panel, including the more recent 2014 clade 3C2.a HA (Figure 3).

The 019-10117-3C06 mAb originates from the IGHV1-69*01 germline and has 29 heavy-chain somatic mutations relative to germline, 16 of which result in coding changes (Figure S2). Previous studies have identified IGHV1-69 mAbs targeting the H2 RBS (Xu et al., 2013), H3 RBS (Lee et al., 2014), and HA stalk (Ekiert et al., 2009; Kashyap et al., 2008; Pappas et al., 2014; Sui et al., 2009). 019-10117-3C06 has a 19 amino acid HCDR3 (Figure S2), which is a similar length to that of previously reported H1 RBS mAbs such as CH65 and others (Schmidt et al., 2015b; Whittle et al., 2011). The 019-10117-3C06 mAb also has a JH6 gene segment, which has been reported as a common feature of mAbs recognizing the H1 RBS (Schmidt et al., 2015b) but lacks the dipeptide motif that is present in many previously described H1 and H3 RBS mAbs (Lee et al., 2014; Schmidt et al., 2015b).

Characterization of a Broadly Reactive HA RBS Targeting mAb

We used deep mutational scanning (Doud et al., 2017; Doud et al., 2018; Lee et al., 2018) to unbiasedly identify HA amino acid substitutions that could facilitate viral escape from the 019-10117-3C06 mAb. For these experiments, we used a library of A/Perth/16/2009 HAs (which is antigenically similar to A/Victoria/210/2009) that had every possible single amino acid substitution in HA. We grew this virus library in the presence or absence of the 019-10117-3C06 mAb. For comparison, we completed parallel experiments in which we grew the virus library in the presence of an HA antigenic site B mAb (024-10128-3C04) that did not have broad reactivity. The narrowly reactive 024-10128-3C04 HA site B mAb selected viruses with substitutions in residues 159, 160, 192, and 193, which are located in HA antigenic site B (Figure 4A). Interestingly, the broadly reactive 019-10117-3C06 mAb also selected for viruses with HAs that had substitutions in antigenic site B (residues 159, 160, 193), as well as HAs that had substitutions in the adjacent antigenic site A (residue 145) (Figure 4B). Viruses with substitutions in conserved residues of the HA RBS were not enriched in these experiments, which is expected since viruses with HA RBS substitutions do not usually replicate efficiently.

To further characterize HA amino acid substitutions identified in our deep mutational scanning experiments, we completed neutralization assays using viruses engineered to express A/Perth/16/2009 HAs with the N145D, F159G, F159S, K160T, or I192E substitutions. As expected, site B substitutions dramatically reduced neutralization of the narrowly reactive 024-10128-3C04 mAb (Figure 4C). Substitutions at residues 145, 159, and 160 also reduced neutralization of the 019-10117-3C06 mAb, but importantly, all mutant viruses tested were still moderately neutralized by this mAb (Figure 4D). As a control, we also tested binding of the 028-10134-4F03 mAb, which binds lower on the HA head, against the 024-10128-3C04 and 019-10117-3C06 escape mutants. As expected, this mAb neutralized these mutants equivalently (Figure 4E). These data indicate that viruses can accommodate HA substitutions that decrease neutralization of the broadly reactive 019-10117-3C06 mAb, but that these substitutions do not allow complete escape from this antibody.

We hypothesized that the 019-10117-3C06 mAb is able to partially recognize viruses with HA antigenic site B substitutions by engaging conserved residues in the HA RBS. To test this hypothesis, we measured antibody binding to HAs that had a K160T HA substitution that introduces a glycosylation site in HA antigenic site B (Zost et al., 2017) with and without an additional Y98F substitution. HA residue 98 is located at the base of the RBS and interacts directly with sialic acid (Weis et al., 1988; Figure 2B). Previous studies have shown that the Y98F substitution prevents HA binding to sialic acid without affecting the overall structure of HA (Bradley et al., 2011; Martín et al., 1998; Whittle et al., 2014). The 019-10117-3C06 mAb had reduced binding to HAs that had either the K160T or the Y98F HA substitutions, and the binding of this mAb was further reduced to HAs that had both of these substitutions (Figure 5A). As a control, we also tested binding of the narrow 024-10128-3C04 mAb to HAs that had the K160T substitution with or without the Y98F substitution. Unlike the broadly reactive 019-10117-3C06 mAb, the narrow 024-10128-3C04 mAb failed to efficiently bind to HAs that had K160T, with or without the Y98F substitution (Figure 5B). This finding suggests that partial binding of the 019-10117-3C06 mAb to HAs with antigenic site B substitutions depends on interactions with the conserved Y98 residue in the RBS.

Broad cross-reactivity of RBS mAbs often requires bivalent binding (Ekiert et al., 2012; Hong et al., 2013; Lee et al., 2012). We used biolayer interferometry (BLI) to measure the binding of 019-10117-3C06 IgG and Fab to A/Perth/16/2009 HA and the antigenically distant A/Hong Kong/1/1968 HA. Both 019-10117-3C06 IgG and Fab bound strongly to A/Perth/16/2009 HA (Figures 5C and 5D). The 019-10117-3C06 IgG, but not the 019-10117-3C06 Fab, bound to the antigenically distant A/Hong Kong/1/1968 HA (Figures 5E and 5F). These data suggest that the 019-10117-3C06 mAb relies on bivalent binding in order to maintain broad cross-reactivity with H3 HAs.

Some Individuals Have High Levels of Broadly Reactive HA RBS-Targeting Antibodies

We next completed ELISAs to determine whether HA RBS-targeting antibodies were present at high frequencies in the sera of donors pre- and post-vaccination. We tested sera from 28 individuals vaccinated during the 2010–2011 season, including 10 of the 13 donors

that were used to generate mAbs. We tested sera antibody binding to ELISAs coated with A/Victoria/210/2009 HA, A/Victoria/210/2009 HA with a Y98F RBS substitution, A/Hong Kong/4801/2014 HA (a drifted strain with HA antigenic site B substitutions), and A/Hong Kong/4801/2014 HA with a Y98F RBS substitution. Most serum samples had antibodies that bound similarly to HAs with and without the Y98F substitution (Figure S3). However, serum antibodies from one donor (019-10117) had weaker binding to HAs with the Y98F substitution (Figure 6). Notably, the broadly reactive 019-10117-3C06 HA RBS-targeting mAb was derived from this same donor. This donor had Y98F-sensitive antibodies both before and after vaccination, and the proportion of Y98F-sensitive antibodies decreased slightly after vaccination (Figure 6). Just like the 019-10117-3C06 mAb, polyclonal serum antibodies from this donor partially bound to the drifted A/Hong Kong/4801/2014 HA and binding of these antibodies to this HA was reduced by the Y98F HA substitution.

Evaluation of HA RBS-Targeting Antibodies in Years with Seasonal Influenza Vaccine Mismatches

It is possible that HA RBS-directed antibodies might be an important part of polyclonal neutralizing antibody responses during influenza seasons with substantial antigenic mismatches between vaccine strains and circulating strains. In order to measure serum levels of Y98F-sensitive antibodies, we developed an absorption-based assay, in which we incubated serum antibodies with 293F cells expressing HAs with or without the Y98F substitution and then completed *in vitro* neutralization assays with HA-absorbed serum fractions. In these assays, antibodies that are sensitive to the Y98F HA substitution are not absorbed by 293F cells that express the Y98F HA.

To validate the assay, we tested the broadly reactive 019-10117-3C06 HA RBS-targeting mAb and a broadly reactive 041–10047-1C04 mAb that does not make contact with the HA RBS. For these experiments, we tested binding and neutralization of the A/Hong Kong/4801/2014 viral strain. Absorption with 293F cells expressing the WT A/Hong Kong/4801/2014 HA completely removed both antibodies (Figure 7A). Conversely, absorption with 293F cells expressing A/Hong Kong/4801/2014 HA with the Y98F substitution removed the 041-10047-1C04 mAb but did not remove the HA RBS-targeting 019-10117-3C06 mAb (Figure 7A).

We next characterized serum antibodies from 21 individuals that received the 2015–2016 seasonal vaccine. We studied antibody responses elicited against the 2015–2016 vaccine because the H3N2 component of this vaccine was mismatched compared to A/Hong Kong/2014-like H3N2 viruses that circulated that season (Figure 7B). We first completed standard neutralization assays using the 2015–2016 vaccine strain (A/Switzerland/9715293/2013) and the antigenically distinct A/Hong Kong/4801/2014 virus. As expected, vaccine-elicited antibodies did not neutralize the mismatched A/Hong Kong/4801/2014 virus as efficiently as the vaccine strain (Figure 7C). However, the vaccine strain did boost serum antibody responses against A/Hong Kong/4801/2014 in some individuals. In order to determine whether these cross-reactive antibodies were targeting conserved residues of the HA RBS, we completed absorption fractionation assays using serum from the same 21 vaccinated donors. For these experiments, we quantified the fraction of A/Hong Kong/4801/2014-

reactive antibodies that were sensitive to the HA Y98F substitution. We detected Y98F HA-sensitive A/Hong Kong/4801/2014-reactive antibodies in only 4 of 21 vaccinated donors (Figures 7D-7G; Figure S4). We found that absorption with A/Hong Kong/4801/2014 WT HA depleted serum neutralizing antibodies, while absorption with A/Hong Kong/4801/2014 HA-Y98F left an absorption-resistant fraction of neutralizing antibodies. Some of these individuals had detectable RBS-targeting antibodies before vaccination (Figures 7D-7G). ELISA quantification confirmed that the antibodies remaining after A/Hong Kong/4801/2014 HA-Y98F absorption bound to the A/Hong Kong/4801/2014 WT but not to the A/Hong Kong/4801/2014 HA-Y98F HA, which indicates that this absorption-resistant fraction contained RBS-targeting antibodies (Figure S5). These data indicate that Y98F-sensitive HA RBS antibodies are only detected in the serum of a limited number of vaccines and are not efficiently elicited by vaccination in most individuals.

DISCUSSION

A greater understanding of the specificity of anti-influenza virus antibody responses in humans is useful for rationally designing new universal influenza vaccine antigens. We began this study by antigenically charactering 33 H3 mAbs isolated from humans receiving a seasonal influenza vaccine. We found that the majority of these mAbs targeted epitopes in variable regions of the HA head. Some of these mAbs targeted conserved residues in the HA RBS but were not broadly reactive since they were also highly sensitive to HA substitutions in adjacent variable antigenic sites. However, we identified one HA RBS-targeting mAb that had exceptional breadth. This mAb (019-10117-3C06) was also moderately sensitive to HA substitutions in adjacent variable antigenic sites but was able to partially bind to antigenically drifted HAs.

Most HA RBS-targeting antibodies are not broadly reactive because their large binding footprints lead to contacts outside of the narrow RBS. However, several broadly reactive HA RBS-targeting antibodies have been identified (Ekiert et al., 2012; Krause et al., 2011; Lee et al., 2012, 2014; McCarthy et al., 2018; Schmidt et al., 2015b; Tsibane et al., 2012; Whittle et al., 2011; Winarski et al., 2015; Xu et al., 2013). A common feature of these broadly reactive HA RBS-targeting antibodies is that most have relatively long HCDR3s, which allow them to minimize contacts on the rim of the RBS and maximize contacts with conserved RBS residues. Our study highlights that HA RBS-targeting antibodies can be broadly reactive even if they are moderately sensitive to substitutions in conventional antigenic sites near the RBS. Similar to the previously published F045-092 mAb (Lee et al., 2014), the 019-10117-3C06 mAb from our study is affected by substitutions in HA antigenic site B (Figure 2) but maintains binding to diverse H3 HAs across almost 50 years (Figure 3) likely through bivalent binding and multiple contacts with conserved residues in the RBS.

Our study indicates that current vaccines do not efficiently elicit broadly reactive HA RBS-targeting antibodies in most individuals. We examined a cohort that received an antigenically mismatched vaccine and, although some of the donors mounted a cross-reactive antibody response, most of these cross-reactive HA antibodies were not Y98F sensitive. It is worth noting that we only measured RBS antibodies that were sensitive to the Y98F HA substitution, and it is possible that current vaccines elicit other types of RBS antibodies that

are not Y98F sensitive. Most conventional vaccine antigens are prepared in fertilized chicken eggs (Grohskopf et al., 2018) and contemporary egg-adapted H3N2 vaccine strains have substitutions in or near the RBS that allow more efficient viral growth in chicken eggs (Wu et al., 2017; Zost et al., 2017). We speculate that vaccines that do not have adaptive mutations in the HA RBS might be better at eliciting antibodies targeting epitopes in the HA RBS of circulating viral strains. Future studies should determine whether vaccine antigens that are not prepared in eggs are better able to elicit broadly reactive HA RBS-targeting antibodies.

The challenge, of course, is designing new vaccine antigens that are able to preferentially elicit antibodies like 019-10117-3C06 and identifying the concentration of these antibodies needed for protection. Recent work has sought to selectively elicit broadly reactive HA head antibody responses through the use of “mosaic” nanoparticles that display antigenically diverse HA RBS domains on the same nanoparticle (Kanekiyo et al., 2019). This vaccination strategy might selectively activate naive B cells targeting the HA RBS and recall broadly reactive memory B cells in secondary responses. One key challenge moving forward will to be determine whether unique prior exposure histories facilitate the development of broadly reactive HA RBS-targeting antibodies. In our study, we identified some donors with high levels of these antibodies in polyclonal sera. In the case of donor 019-10117, these antibodies were already at high levels in polyclonal sera before vaccination. Is there something genetically unique about donor 019-10117 or does that donor have an unusual exposure history that gave rise to a B cell response highly focused on conserved residues within the HA RBS? While some studies have generated unmutated common ancestors and inferred the immunogenic stimuli for broadly reactive antibody lineages targeting the HA RBS (McCarthy et al., 2018; Schmidt et al., 2015a), we know little about how prior immune history and repeated exposures influence the development of HA RBS antibodies. In the field of HIV, major efforts have been made to study antibody-virus co-evolution and the development of broadly neutralizing antibody specificities in chronically infected individuals, with the goal of identifying HIV envelope proteins that favor the development of broadly neutralizing antibody responses (Bonsignori et al., 2017; Landais et al., 2017; Rantalainen et al., 2018). Longitudinal studies in human cohorts could address similar questions for influenza viruses, with the potential to fill in gaps in our understanding of how antibody responses are elicited, recalled, and altered by infection and vaccination (Erbelding et al., 2018).

STAR★METHODS

LEAD CONTACT AND MATERIALS AVAILABILITY

All unique/stable reagents generated in this study are available from the Lead Contact with a completed Materials Transfer Agreement. Further information and requests for resources and reagents should be directed to and will be fulfilled by the Lead Contact, Scott E. Hensley (hensley@pennmedicine.upenn.edu).

EXPERIMENTAL MODEL AND SUBJECTS DETAILS

Human Subjects and Serum Collection—All experiments involving humans were approved by the institutional review boards of the Wistar Institute, University of Pennsylvania, and the University of Chicago. Informed consent was obtained from all individuals. Experiments using deidentified human sera and mAbs were conducted at the University of Pennsylvania. For individuals from whom mAbs were isolated, serum was collected at the time of vaccination and 21 days post-vaccination. Donors ranged from 22 to 41 years of age. For individuals from the 2015-16 vaccination cohort, serum samples were collected at the time of vaccination and four weeks post-vaccination. Donors ranged from 25 to 62 years of age. For assays using foci-reduction neutralization tests, serum samples were treated with receptor-destroying enzyme (RDE) for 2 hr at 37°C. Following treatment, the enzyme was heat-inactivated by incubation at 55°C.

Cell Lines—Madin-Darby Canine Kidney (MDCK) cells were maintained in Minimal Essential Medium (MEM) supplemented with 10% fetal bovine serum (FBS). MDCK-SIAT1 cells, a cell line derived from the MDCK line that overexpresses the SIAT1 sialyltransferase (Matrosovich et al., 2003), were also maintained in MEM + 10% FBS. MDCK-SIAT1-TMPRSS2 cells were generated by transducing the parental MDCK-SIAT1 line with a lentiviral vector encoding the TMPRSS2 gene (Lee et al., 2018). These cells were maintained in Dulbecco's Modification of Minimal Essential Medium (DMEM) supplemented with 10% FBS. Adherent 293T cells were also maintained in DMEM + 10% FBS. All adherent cells were grown in tissue-culture flasks at 37°C in 5% CO_2. Suspension-adapted 293F cells were maintained in Freestyle 293F Expression Medium at 37°C in 8% CO_2. Particular media for different experiments are denoted in the methods description for each experiment.

METHOD DETAILS

Monoclonal Antibody Isolation and Purification—mAbs were isolated from human donors as previously described (Smith et al., 2009). Briefly, plasmablasts were single-cell sorted from peripheral blood mononuclear cells collected from donors seven days after vaccination with the 2010-2011 or 2011-2012 vaccines containing the H3N2 vaccine strain A/Victoria/210/2009. Single-cell RT-PCR was used to amplify V_H and V_L chains, which were cloned into human IgG expression vectors. mAbs were produced by transfecting 293T cells with plasmids encoding heavy and light chains and mAbs were purified using protein A/G magnetic beads.

Hemagglutination-Inhibition (HAI) Assays—mAbs were serially diluted two-fold in a 96-well round-bottom plate in 50 μL total volume of phosphate-buffered saline (PBS). After serial dilution, four agglutinating doses of virus in a total volume of 50 μL PBS were added to each well. Turkey erythrocytes (12.5 μL of a 2.0% [vol/vol] solution) were added and the sera, virus, and erythrocytes were gently mixed. After 1 hr at room temperature, plates were scanned and titers were determined as the lowest concentration of monoclonal antibody that fully inhibited agglutination. HAI assays were performed in duplicate on separate days.

Microneutralization (MN) Assays—mAbs were serially diluted two-fold in round-bottom 96-well plates in 50 μL serum-free Minimal Essential Medium (MEM). 50 μL of MEM containing 100 $TCID_{50}$ of virus was added to serially diluted mAbs and the mAb-virus mixtures were incubated for 30 min at room temperature. Following incubation, the mAb-virus mixtures were added to confluent monolayers of MDCK cells in 96-well plates and incubated for 1 hr at 37°C. After incubation, the virus-antibody mixtures were removed and cells were washed with 180 μL MEM. After washing, serial dilutions of each mAb were added back to cell monolayers in infection media (MEM containing HEPES buffer, gentamycin, and 1 μg/mL TPCK-treated trypsin). The cells were incubated for 3 days and neutralization titers were determined as the lowest concentration of mAb that prevented cell death. MN assays were completed in duplicate on separate days.

VLP Antigenic Mapping ELISAs—Point mutants of A/Victoria/210/2009 HA were generated in a codon-optimized HA gene by site directed mutagenesis. Virus-like particles (VLPs) were generated by transfecting 293T cells with each point mutant along with plasmids encoding HIV gag, the NA from A/Puerto Rico/8/1934, and a human-airway trypsin-like protease (HAT). Supernatants from transfected 293T cells were collected 3 days following transfection and were concentrated by centrifugation at 19,000 rpm (65,096 x g) in an SW-28 rotor using a 20% sucrose cushion. VLP pellets were resuspended in PBS and stored at 4°C. ELISA plates were coated with HA-normalized point mutant VLPs diluted in PBS or just PBS as a background control and stored overnight at 4°C. The following day, plates were blocked with a 3% w/vol solution of bovine-serum albumin (BSA) in PBS for 2 hr. After blocking, plates were washed five times with distilled water and two-fold serial dilutions of each mAb were added to plates in a 1% w/vol solution of BSA in PBS. After 2 hr of incubation, plates were washed and a peroxidase-conjugated goat anti-human secondary antibody was added in a 1% w/vol solution of BSA in PBS. After incubation for 1 hr, plates were washed and 50 μL of TMB substrate was added to each well. The TMB reaction was quenched by addition of 25 μL 250 mM HCl and absorbance at 450nm was measured using a plate reader. In order to generate antigenic maps, one-site specific binding curves were fit to the data in GraphPad Prism software and the maximal binding (B_{max}) was determined for each mAb. To generate antigenic maps from the ELISA data, we first selected the lowest mAb concentration that still gave at least 90% of the B_{max} signal. At this dilution, background signal was subtracted and signal for each point mutant was normalized to the A/Victoria/210/2009 WT HA VLP signal. Antigenic mapping ELISAs were conducted for each mAb in duplicate on separate days, and the resulting values were averaged and represented as a heatmap.

Seasonal H3N2 Strain ELISAs—A panel of seasonal H3N2 viruses spanning 1968 to 2013 was expanded by propagation in embryonated chicken eggs. Due to egg-adaptive mutations a 2014 strain for the seasonal panel was propagated in MDCK-SIAT1 cells. Supernatants containing virus were clarified by centrifugation and concentrated by ultracentrifugation at 20,000 rpm (71,935 x g) in an SW-28 rotor. Viral pellets were resuspended at 4°C overnight in PBS. Viruses were chemically inactivated using 0.1% (vol/vol) B-Propiolactone (BPL; Sigma Aldrich) in PBS containing 0.1M HEPES. Viruses were inactivated by incubation with BPL at 4°C overnight followed by incubation at 37°C for 90

min. To measure mAb binding to the seasonal panel, ELISA plates were coated overnight at 4°C with standardized amounts of concentrated virus in PBS. The following day, ELISAs were performed and antigenic maps were generated as described for the VLP antigenic mapping. Seasonal H3N2 strain mapping ELISAs were conducted for each mAb in triplicate on separate days, and the resulting values were averaged and represented as a heatmap.

Recombinant HA Production—Codon optimized HA genes for A/Hong Kong/4801/2014 WT and Y98F were cloned into expression vectors and the transmembrane was removed and replaced with the foldon trimerization domain from T4 fibritin, an AviTag site-specific biotinylation sequence, and a hexahistidine tag, as previously described (Whittle et al., 2014). Recombinant HAs were produced by transfecting 293F suspension cells with plasmids encoding HA and a membrane-bound NA lacking a His tag. After four days, the supernatant was clarified by centrifugation and the HA proteins were purified by Ni-NTA affinity chromatography. Recombinant HAs for mAb affinity measurements were produced in insect cells using a baculovirus expression system and purified by Ni-NTA affinity chromatography.

Biolayer Interferometry Binding Assay—An Octet Red instrument (ForteBio, Menlo Park, CA) was employed for biolayer interferometry binding (BLI) assays. Baculovirus-expressed recombinant HA was expressed and purified as described previously (Ekiert et al., 2011). For this, High Five insect cells (Invitrogen) were infected with baculoviruses encoding each recombinant HA fused to a trimerization domain and a C-terminal his tag. HAs were purified from culture supernatants using Ni-NTA affinity chromatography. 019-10117-3C06 Fab was generated from 019-10117-3C06 IgG using papain cleavage as previously described (Bianchi et al., 2018). For this, full-length IgG was digested using papain-agarose resin (Thermo Fisher Scientific) and Fab was purified by size exclusion chromatography. Recombinant HA (uncleaved HA0) at a concentration of 50 μg/mL in 1 x kinetics buffer (1 x PBS with 0.01% BSA and 0.002% Tween 20) was loaded onto the streptavidin (SA) Biosensors. Binding kinetics were measured against the indicated 019-10117-3C06 IgG or Fab at 125 nM, 250 nM, 500 nM, and 1,000 nM. The assay consisted of five steps: (1) baseline: 60 s with 1x kinetics buffer; (2) loading: 10 mins with biotinylated HA; (3) baseline: 60 s with 1 × kinetics buffer; (4) association: 120 s with purified IgG or Fab; and (5) dissociation: 120 s with 1 x kinetics buffer. The data were fit with a 1:1 binding model for Fab and heterogenous ligand model for IgG to estimate the K_d.

Mutational Antigenic Profiling—We performed mutational antigenic profiling of mAbs 024-10128-3C04 and 019-10117-3C06 against A/Perth/16/2009 (H3N2) HA mutant virus libraries (Lee et al., 2018) using a previously described protocol (Doud et al., 2017). We selected two biological replicate libraries by incubating 1e6 $TCID_{50}$ mutant viruses with neutralizing concentrations of antibody at 37°C for 1.5 hours. For antibody 024-10128-3C04, we neutralized mutant viruses with 0.1, 0.25, 0.2, 0.65, or 1 μg/ml antibody, and for 019-10117-3C06, we neutralized with 0.1, 0.2, 0.25, 0.55, 0.7, or 1 μg/ml antibody. We also included a mock selection condition where virus library was incubated with Influenza Growth Media (IGM, consisting of Opti-MEM supplemented with 0.01% heat-inactivated FBS, 0.3% BSA, 100 U of penicillin per milliliter, 100 μg of streptomycin

per milliliter, and 100 μg of calcium chloride per milliliter). Following antibody incubation, we infected 2.5e5 MDCK-SIAT1-TMPRSS2 cells (Lee et al., 2018) with the virus-antibody mixture, then 2 hours post-infection aspirated off the inoculum, washed the cells with 1 mL PBS, then replaced the media with fresh IGM. Approximately 15 hours post-infection, we extracted, reverse-transcribed, and PCR amplified the viral RNA. We used the barcoded-subamplicon sequencing approach described in Lee et al., 2018 to deep sequence at high-accuracy. We then used dms_tools2 (v2.3.0) (Bloom, 2015) to analyze the deep sequencing results.

ELISAs with Human Sera—ELISA plates were coated the day prior with 0.5 μg/mL recombinant HAs (A/Hong Kong/4801/2014 WT, A/Hong Kong/4801/2014 Y98F, or a PBS background control) and blocked for 2 hr on the day of the experiment with a 3% BSA in PBS solution. After washing the plates three times with wash buffer containing 0.5% Tween20 (vol/vol) in PBS (PBS-T), serially diluted serum samples were added to the ELISA plates and incubated for 2 hr. After incubation, plates were washed three times with PBS-T and a peroxidase-conjugated goat anti-human secondary antibody diluted in 1% BSA in PBS was added. After 1 hr of incubation with the secondary antibody, plates were washed three times with PBS-T and 50 μL of a TMB substrate was added to each well. 25 μL of 250mM HCl was used to quench the reaction and the absorbance at 450 nm was measured using a plate reader. Background signal at each dilution was subtracted for each serum sample and one site – specific binding curves were fit to the data using GraphPad Prism. Human sera ELISAs were performed in triplicate on separate days.

Competition ELISAs—ELISA plates were coated the day prior with BPL-inactivated A/Hong Kong/1/1968 virus and blocked for 2 hr with a 3% BSA in PBS solution. After washing the plates five times with distilled water, serial dilutions of the anti-H3 mouse mAb F49 or the control mouse mAb C179 in 1% BSA in PBS were added to the plate and incubated for 2 hr at RT. After incubation, human mAbs were added directly to the plates at a fixed concentration in 1% BSA in PBS and incubated for 1 hr at RT. Plates were then washed five times with distilled water and peroxidase-conjugated anti-human secondary antibody was added and incubated for 1 hr. Following incubation with secondary antibodies, plates were washed five times with distilled water, TMB substrate was added, and the reaction was quenched with HCl. The absorbance at 450 nm was quantified using a plate reader and competition at each dilution was normalized to the control mAb C179.

Foci-Reduction Neutralization Tests (FRNTs)—mAbs or RDE-treated serum samples were serially diluted in 96-well plates in a total volume of 50 μL. Approximately 200-300 focus-forming units of virus in 50 μL were added to each well and the virus-absorbed sera mixture was incubated for 1 hr at room temperature. After incubation, the virus-sera mixture was added to confluent monolayers of MDCK-SIAT1 cells and incubated for 1 hr at 37°C. After incubation, cell monolayers were washed with 180 μL serum-free MEM and an overlay medium containing HEPES, gentamycin, and 0.5% methylcellulose was added. The cell monolayers were incubated for 18 hr, after which the overlay was removed and the cells were fixed at 4°C for 2 hr using an aqueous solution of 4% paraformaldehyde (vol/vol). After fixation, cell monolayers were permeabilized using 0.5% Triton X-100 in PBS (vol/

vol). After fixation and permeabilization, monolayers were blocked with a solution of 5% fat-free milk in PBS for 1 hr. After blocking, a mouse anti-nucleoprotein antibody was added in 5% milk/PBS for 1 hr. After the primary incubation, a peroxidase-conjugated goat anti-mouse secondary antibody in 5% milk/PBS was added for 1 hr. After incubation with the secondary antibody, monolayers were stained using a TMB substrate and foci were imaged and quantified using an ELISpot reader. For staining, plates were washed with distilled water between each step. Percentage of infection was determined relative to wells that did not receive any serum or antibody. FRNT90 titer values are reported as the concentration of serum or mAb that reduced the numbers of foci by at least 90%.

Absorption-Neutralization and Absorption-ELISA Assays—Two days prior to experiments, 293F suspension cells were transfected using 293fectin with plasmids expressing A/Hong Kong/4801/2014 WT HA, A/Hong Kong/4801/2014 Y98F HA, or a mock transfection control containing no plasmid or transfection reagent. On the day of the experiment, transfected cells were pelleted by centrifugation, washed twice with 293F media, and resuspended at the desired volume. In the case of absorption-neutralization assays, RDE-treated serum samples were diluted in 293F media at a dilution of 1:10 and split into three fractions for the three absorption conditions. An equivalent volume of 293F media containing approximately 8×10^6 transfected cells/absorption reaction was added to each diluted serum sample and the samples were mixed by shaking for 1 hr at room temperature. After incubation, the cells were pelleted by centrifugation and the supernatant was transferred and re-centrifuged to clarify. Absorbed supernatant containing the sera was then serially diluted in 96-well round-bottom plates in serum-free MEM and FRNT assays were conducted as described. Absorption-neutralization experiments were completed in triplicate on separate days. In the case of absorption-ELISA assays, serum samples were diluted in 293F media at an initial dilution of 1:50 and split into three fractions for the three absorption conditions. Transfected cells were added and absorption of serum antibodies was carried out as described above. Following absorption, absorbed serum samples were serially diluted at a starting dilution of 1:500 (factoring in absorption volume) in 1% BSA w/vol in PBS and ELISAs were performed as described above.

For ELISA data, background antibody binding for each sample at each dilution was subtracted and one-site specific binding curves were fit to the data using GraphPad Prism software. The area under the curve (AUC) was calculated for each curve. For neutralization data, foci in positive control wells which did not receive any serum or antibody were used to determine percentage of infection. Neutralization data are represented as percentage of neutralization at each dilution of serum, and a four-parameter [inhibitor] versus dose-response curve was fit to each set of neutralization data using GraphPad Prism, with top and bottom values constrained to 100 and 0, respectively. Assays were performed at least three times on separate days. For both absorption-neutralization and absorption-ELISA experiments, the RBS mAb 019-10117 3C06 mAb and the 041-10047 1C04 mAb (which targets the lower HA head region) were initially diluted to a concentration of 32 μg/mL in 293F media before adding to cells. For absorption-neutralization experiments, the starting concentration for each mAb absorption condition in the FRNT was 16 μg/mL. For

absorption-ELISA experiments, the starting concentration for each mAb absorption condition in the ELISA was 3.2 μg/mL.

QUANTIFICATION AND STATISTICAL ANALYSIS

Titer values for neutralization and ELISA experiments are reported as geometric mean and geometric SD, geometric mean and geometric 95% CI, or mean ± SEM as noted in each figure legend. For statistical analysis, the statistical tests used and the significance thresholds are described in the legend of each figure. Statistical analyses of differences between mAb neutralization (FRNT) titers against the WT and each mutant virus were completed using a one-way ANOVA with Dunnett's test for multiple comparisons. To determine whether individuals had lower neutralization titers to the circulating strain A/Hong Kong/4801/2014 compared with the vaccine strain A/Switzerland/9715293/2013 we used the paired, nonparametric Friedman test with correction for multiple comparisons. For absorption-ELISA experiments, the area under the curve (AUC) was determined for each experimental condition and the triplicate AUC values for the WT absorption condition and the Y98F mutant absorption condition were compared using an unpaired Student's t test. All statistical analysis was performed in GraphPad Prism software.

DATA AND CODE AVAILABILITY

The published article includes all data generated or analyzed during the study. The sequencing results from deep mutational scanning experiments are available under BioSample accessions on the NIH Sequence Read Archive: SAMN10183083 and SAMN10183146 (for the antibody- selected libraries and selection controls, respectively). The computer code for analyzing the data are at https://github.com/jbloomlab/Perth2009-HA_mAb_MAP. Sequences of VH and VL genes for mAbs are deposited on GenBank: MH205211, MH205413, KM603994, MN483379-MN483441.

Supplementary Material

Refer to Web version on PubMed Central for supplementary material.

ACKNOWLEDGMENTS

This work was supported by the National Institute of Allergy and Infectious Diseases (1R01AI113047, S.E.H.; 1R01AI108686, S.E.H.; 1K99AI139445, N.C.W.; CEIRS HHSN272201400005C, P.C.W., J.D.B., and S.E.H.; 2T32AI007324, S.J.Z.). J.D.B. and S.E.H. hold Investigators in the Pathogenesis of Infectious Disease Awards from the Burroughs Wellcome Fund. C.-C.D.L. is sponsored by an Academia Sinica Fellowship, Academia Sinica, Taiwan.

REFERENCES

Amit AG, Mariuzza RA, Phillips SE, and Poljak RJ (1986). Three-dimensional structure of an antigen-antibody complex at 2.8 A resolution. Science 233, 747–753. [PubMed: 2426778]

Angeletti D, and Yewdell JW (2018). Understanding and Manipulating Viral Immunity: Antibody Immunodominance Enters Center Stage. Trends Immunol. 39,549–561. [PubMed: 29789196]

Bianchi M, Turner HL, Nogal B, Cottrell CA, Oyen D, Pauthner M, Bastidas R, Nedellec R, McCoy LE, Wilson IA, et al. (2018). Electron-microscopy-based epitope mapping defines specificities of polyclonal antibodies elicited during HIV-1 BG505 envelope trimer immunization. Immunity 49, 288–300. [PubMed: 30097292]

Bloom JD (2015). Software for the analysis and visualization of deep mutational scanning data. BMC Bioinformatics 16, 168. [PubMed: 25990960]

Bonsignori M, Liao HXX, Gao F, Williams WB, Alam SM, Montefiori DC, and Haynes BF (2017). Antibody-virus co-evolution in HIV infection: paths for HIV vaccine development. Immunol. Rev 275, 145–160. [PubMed: 28133802]

Bradley KC, Galloway SE, Lasanajak Y, Song X, Heimburg-Molinaro J, Yu H, Chen X, Talekar GR, Smith DF, Cummings RD, and Steinhauer DA (2011). Analysis of influenza virus hemagglutinin receptor binding mutants with limited receptor recognition properties and conditional replication characteristics. J. Virol 85, 12387–12398. [PubMed: 21917953]

Chambers BS, Parkhouse K, Ross TM, Alby K, and Hensley SE (2015). Identification of Hemagglutinin Residues Responsible for H3N2 Antigenic Drift during the 2014-2015 Influenza Season. Cell Rep. 12, 1–6. [PubMed: 26119736]

Doud MB, Hensley SE, and Bloom JD (2017). Complete mapping ofviral escape from neutralizing antibodies. PLoS Pathog. 13, e1006271. [PubMed: 28288189]

Doud MB, Lee JM, and Bloom JD (2018). How single mutations affect viral escape from broad and narrow antibodies to H1 influenza hemagglutinin. Nat. Commun 9, 1386. [PubMed: 29643370]

Ekiert DC, Bhabha G, Elsliger MA, Friesen RH, Jongeneelen M, Throsby M, Goudsmit J, and Wilson IA (2009). Antibody recognition of a highly conserved influenza virus epitope. Science 324, 246–251. [PubMed: 19251591]

Ekiert DC, Friesen RH, Bhabha G, Kwaks T, Jongeneelen M, Yu W, Ophorst C, Cox F, Korse HJ, Brandenburg B, et al. (2011). A highly conserved neutralizing epitope on group 2 influenza A viruses. Science 333, 843–850. [PubMed: 21737702]

Ekiert DC, Kashyap AK, Steel J, Rubrum A, Bhabha G, Khayat R, Lee JH, Dillon MA, O'Neil RE, Faynboym AM, et al. (2012). Cross-neutralization of influenza A viruses mediated by a single antibody loop. Nature 489, 526–532. [PubMed: 22982990]

Erbelding EJ, Post DJ, Stemmy EJ, Roberts PC, Augustine AD, Ferguson S, Paules CI, Graham BS, and Fauci AS (2018). A Universal Influenza Vaccine: The Strategic Plan for the National Institute of Allergy and Infectious Diseases. J. Infect. Dis 218, 347–354. [PubMed: 29506129]

Giles BM, and Ross TM (2011).A computationally optimized broadly reactive antigen (COBRA) based H5N1 VLP vaccine elicits broadly reactive antibodies in mice and ferrets. Vaccine 29, 3043–3054. [PubMed: 21320540]

Grohskopf LA, Sokolow LZ, Broder KR, Walter EB, Fry AM, and Jernigan DB (2018). Prevention and Control of Seasonal Influenza with Vaccines: Recommendations of the Advisory Committee on Immunization Practices-United States, 2018-19 Influenza Season. MMWR Recomm. Rep 67, 1–20.

Hadfield J, Megill C, Bell SM, Huddleston J, Potter B, Callender C, Sagulenko P, Bedford T, and Neher RA (2018). Nextstrain: real-time tracking of pathogen evolution. Bioinformatics 34, 4121–4123. [PubMed: 29790939]

Hong M, Lee PS, Hoffman RM, Zhu X, Krause JC, Laursen NS, Yoon SI, Song L, Tussey L, Crowe JE Jr., et al. (2013). Antibody recognition of the pandemic H1N1 Influenza virus hemagglutinin receptor binding site.J. Virol 87, 12471–12480. [PubMed: 24027321]

Impagliazzo A, Milder F, Kuipers H, Wagner MV, Zhu X, Hoffman RMB, van Meersbergen R, Huizingh J, Wanningen P, Verspuij J, et al. (2015). A stable trimeric influenza hemagglutinin stem as a broadly protective immunogen. Science 349, 1301–1306. [PubMed: 26303961]

Kanekiyo M, Joyce MG, Gillespie RA, Gallagher JR, Andrews SF, Yassine HM, Wheatley AK, Fisher BE, Ambrozak DR, Creanga A, et al. (2019). Mosaic nanoparticle display of diverse influenza virus hemagglutinins elicits broad B cell responses. Nat. Immunol 20, 362–372. [PubMed: 30742080]

Kashyap AK, Steel J, Oner AF, Dillon MA, Swale RE, Wall KM, Perry KJ, Faynboym A, Ilhan M, Horowitz M, et al. (2008). Combinatorial antibody libraries from survivors of the Turkish H5N1 avian influenza outbreak reveal virus neutralization strategies. Proc. Natl. Acad. Sci. USA 105, 5986–5991. [PubMed: 18413603]

Knossow M, and Skehel JJ (2006). Variation and infectivity neutralization in influenza. Immunology 119, 1–7. [PubMed: 16925526]

Koel BF, Burke DF, Bestebroer TM, van der Vliet S, Zondag GC, Vervaet G, Skepner E, Lewis NS, Spronken MI, Russell CA, et al. (2013). Substitutions near the receptor binding site determine major antigenic change during influenza virus evolution. Science 342, 976–979. [PubMed: 24264991]

Krammer F, Pica N, Hai R, Margine I, and Palese P (2013). Chimeric hemagglutinin influenza virus vaccine constructs elicit broadly protective stalk-specific antibodies. J. Virol 87, 6542–6550. [PubMed: 23576508]

Krause JC, Tsibane T, Tumpey TM, Huffman CJ, Basler CF, and Crowe JE Jr. (2011). A broadly neutralizing human monoclonal antibody that recognizes a conserved, novel epitope on the globular head of the influenza H1N1 virus hemagglutinin. J. Virol 85, 10905–10908. [PubMed: 21849447]

Landais E, Murrell B, Briney B, Murrell S, Rantalainen K, Berndsen ZT, Ramos A, Wickramasinghe L, Smith ML, Eren K, et al.; IAVI Protocol C Investigators; IAVI African HIV Research Network (2017). HIV Envelope Glycoform Heterogeneity and Localized Diversity Govern the Initiation and Maturation of a V2 Apex Broadly Neutralizing Antibody Lineage. Immunity 47, 990–1003. [PubMed: 29166592]

Lee PS, Yoshida R, Ekiert DC, Sakai N, Suzuki Y, Takada A, and Wilson IA (2012). Heterosubtypic antibody recognition of the influenza virus hemagglutinin receptor binding site enhanced by avidity. Proc. Natl. Acad. Sci. USA 109, 17040–17045. [PubMed: 23027945]

Lee PS, Ohshima N, Stanfield RL, Yu W, Iba Y, Okuno Y, Kurosawa Y, and Wilson IA (2014). Receptor mimicry by antibody F045-092 facilitates universal binding to the H3 subtype of influenza virus. Nat. Commun 5, 3614. [PubMed: 24717798]

Lee JM, Huddleston J, Doud MB, Hooper KA, Wu NC, Bedford T, and Bloom JD (2018). Deep mutational scanning of hemagglutinin helps predict evolutionary fates of human H3N2 influenza variants. Proc. Natl. Acad. Sci. USA 115, E8276–E8285. [PubMed: 30104379]

Martín J, Wharton SA, Lin YP, Takemoto DK, Skehel JJ, Wiley DC, and Steinhauer DA (1998). Studies of the binding properties of influenza hemagglutinin receptor-site mutants. Virology 241, 101–111. [PubMed: 9454721]

Matrosovich M, Matrosovich T, Carr J, Roberts NA, and Klenk HD (2003). Overexpression of the alpha-2,6-sialyltransferase in MDCK cells increases influenza virus sensitivity to neuraminidase inhibitors. J. Virol 77, 8418–8425. [PubMed: 12857911]

McCarthy KR, Watanabe A, Kuraoka M, Do KT, McGee CE, Sempowski GD, Kepler TB, Schmidt AG, Kelsoe G, and Harrison SC (2018). Memory B Cells that Cross-React with Group 1 and Group 2 Influenza A Viruses Are Abundant in Adult Human Repertoires. Immunity 48, 174–184.e9. [PubMed: 29343437]

Pappas L, Foglierini M, Piccoli L, Kallewaard NL, Turrini F, Silacci C, Fernandez-Rodriguez B, Agatic G, Giacchetto-Sasselli I, Pellicciotta G, et al. (2014). Rapid development of broadly influenza neutralizing antibodies through redundant mutations. Nature 516, 418–422. [PubMed: 25296253]

Popova L, Smith K, West AH, Wilson PC, James JA, Thompson LF, and Air GM (2012). Immunodominance of antigenic site B over site A of hemagglutinin of recent H3N2 influenza viruses. PLoS ONE 7, e41895. [PubMed: 22848649]

Rantalainen K, Berndsen ZT, Murrell S, Cao L, Omorodion O, Torres JL, Wu M, Umotoy J, Copps J, Poignard P, et al. (2018). Co-evolution of HIV Envelope and Apex-Targeting Neutralizing Antibody Lineage Provides Benchmarks for Vaccine Design. Cell Rep. 23, 3249–3261. [PubMed: 29898396]

Schmidt AG, Do KT, McCarthy KR, Kepler TB, Liao HXX, Moody MA, Haynes BF, and Harrison SC (2015a). Immunogenic Stimulus for Germline Precursors of Antibodies that Engage the Influenza Hemagglutinin Receptor-Binding Site. Cell Rep. 13, 2842–2850. [PubMed: 26711348]

Schmidt AG, Therkelsen MD, Stewart S, Kepler TB, Liao HXX, Moody MA, Haynes BF, and Harrison SC (2015b). Viral receptor-binding site antibodies with diverse germline origins. Cell 161, 1026–1034. [PubMed: 25959776]

Smith K, Garman L, Wrammert J, Zheng NYY, Capra JD, Ahmed R, and Wilson PC (2009). Rapid generation of fully human monoclonal antibodies specific to a vaccinating antigen. Nat. Protoc 4, 372–384. [PubMed: 19247287]

Sui J, Hwang WC, Perez S, Wei G, Aird D, Chen LM, Santelli E, Stec B, Cadwell G, Ali M, et al. (2009). Structural and functional bases for broad-spectrum neutralization of avian and human influenza A viruses. Nat. Struct. Mol. Biol 16, 265–273. [PubMed: 19234466]

Tsibane T, Ekiert DC, Krause JC, Martinez O, Crowe JE Jr., Wilson IA, and Basler CF (2012). Influenza human monoclonal antibody 1F1 interacts with three major antigenic sites and residues mediating human receptor specificity in H1N1 viruses. PLoS Pathog. 8, e1003067. [PubMed: 23236279]

Weis W, Brown JH, Cusack S, Paulson JC, Skehel JJ, and Wiley DC (1988). Structure of the influenza virus haemagglutinin complexed with its receptor, sialic acid. Nature 333, 426–431. [PubMed: 3374584]

Whittle JRR, Zhang R, Khurana S, King LR, Manischewitz J, Golding H, Dormitzer PR, Haynes BF, Walter EB, Moody MA, et al. (2011). Broadly neutralizing human antibody that recognizes the receptor-binding pocket of influenza virus hemagglutinin. Proc. Natl. Acad. Sci. USA 108, 14216–14221. [PubMed: 21825125]

Whittle JRR, Wheatley AK, Wu L, Lingwood D, Kanekiyo M, Ma SS, Narpala SR, Yassine HM, Frank GM, Yewdell JW, et al. (2014). Flow cytometry reveals that H5N1 vaccination elicits cross-reactive stem-directed antibodies from multiple Ig heavy-chain lineages. J. Virol 88, 4047–4057. [PubMed: 24501410]

Wiley DC, Wilson IA, and Skehel JJ (1981). Structural identification of the antibody-binding sites of Hong Kong influenza haemagglutinin and their involvement in antigenic variation. Nature 289, 373–378. [PubMed: 6162101]

Winarski KL, Thornburg NJ, Yu Y, Sapparapu G, Crowe JE Jr., and Spiller BW (2015). Vaccine-elicited antibody that neutralizes H5N1 influenza and variants binds the receptor site and polymorphic sites. Proc. Natl. Acad. Sci. USA 112, 9346–9351. [PubMed: 26170302]

Wu NC, Zost SJ, Thompson AJ, Oyen D, Nycholat CM, McBride R, Paulson JC, Hensley SE, and Wilson IA (2017). A structural explanation for the low effectiveness of the seasonal influenza H3N2 vaccine. PLoS Pathog. 13, e1006682. [PubMed: 29059230]

Xu R, Krause JC, McBride R, Paulson JC, Crowe JE Jr., and Wilson IA (2013). A recurring motif for antibody recognition of the receptor-binding site of influenza hemagglutinin. Nat. Struct. Mol. Biol 20, 363–370. [PubMed: 23396351]

Yassine HM, Boyington JC, McTamney PM, Wei CJJ, Kanekiyo M, Kong WPP, Gallagher JR, Wang L, Zhang Y, Joyce MG, et al. (2015). Hemagglutinin-stem nanoparticles generate heterosubtypic influenza protection. Nat. Med 21, 1065–1070. [PubMed: 26301691]

Yewdell JW (2011). Viva la revolución: rethinking influenza a virus antigenic drift. Curr. Opin. Virol 1, 177–183. [PubMed: 22034587]

Zost SJ, Parkhouse K, Gumina ME, Kim K, Diaz Perez S, Wilson PC, Treanor JJ, Sant AJ, Cobey S, and Hensley SE (2017). Contemporary H3N2 influenza viruses have a glycosylation site that alters binding of antibodies elicited by egg-adapted vaccine strains. Proc. Natl. Acad. Sci. USA 114, 12578–12583. [PubMed: 29109276]

Highlights

- Many mAbs target the RBS of H3 HA, but most are not broadly reactive
- Rare H3 HA RBS mAbs are tolerant of substitutions in adjacent sites
- Broadly reactive H3 HA RBS Abs are not efficiently elicited by vaccines

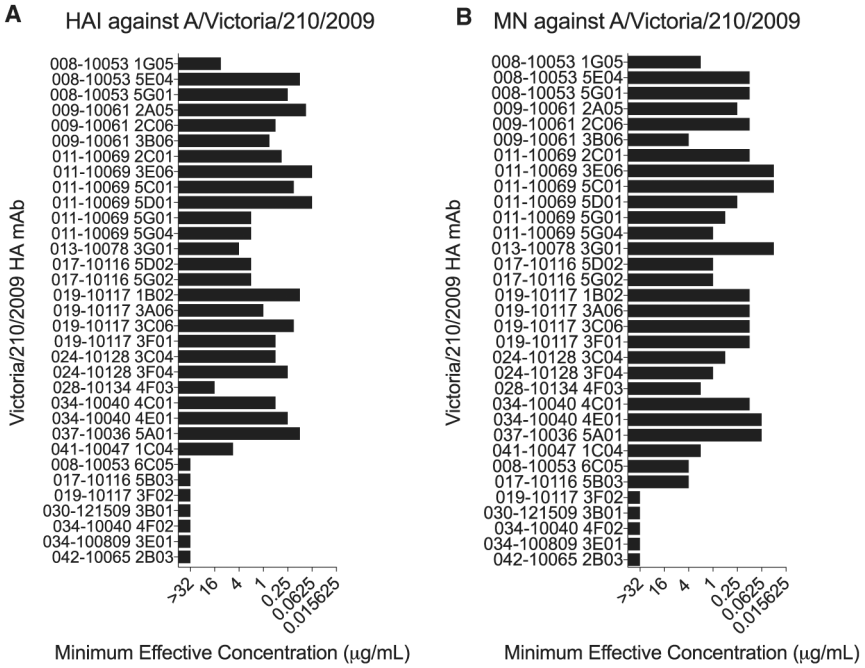

Figure 1. Hemagglutination-Inhibition and Micro-Neutralization Activities of mAbs

(A and B) Hemagglutination-inhibition assays (A) and micro-neutralization assays (B) were completed with each mAb and the A/Victoria/210/2009 vaccine strain. Titers shown are representative of two independent experiments.

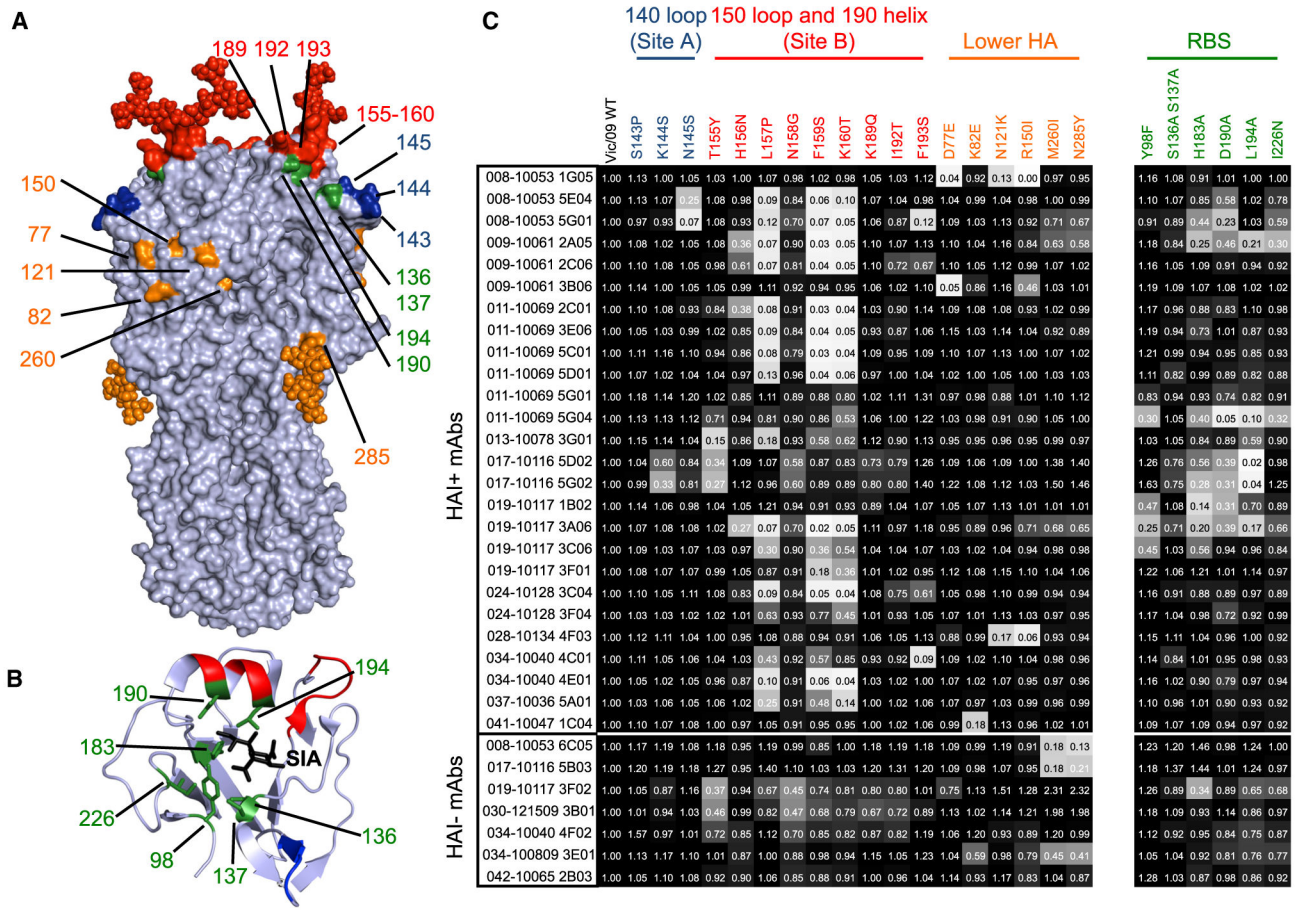

Figure 2. Antigenic Fine Mapping of mAbs

Each mAb was tested for binding to a panel of HAs with different substitutions.

(A and B) The locations of HA substitutions in classic antigenic sites are shown on the H3 trimer (A) (PDB 4O5I), and the locations of RBS substitutions are shown on an H3 HA-sialic acid co-crystal structure (B) (PDB 2YP8). Most substitutions did not affect glycosylation, with the exception of the K160T substitution that results in the addition of a glycan at N158 (shown in red) and the N285Y substitution that results in the loss of a glycan at 285 (shown in orange).

(C) ELISAs were completed using plates coated with VLPs bearing WT HA and HAs with different substitutions. Numbers in squares indicate fraction of binding relative to VLPs with A/Victoria/210/2009 WT HA. Colors of each square range from white (0% of binding to WT) to black (100% of binding to WT). Binding values are the average of two independent experiments.

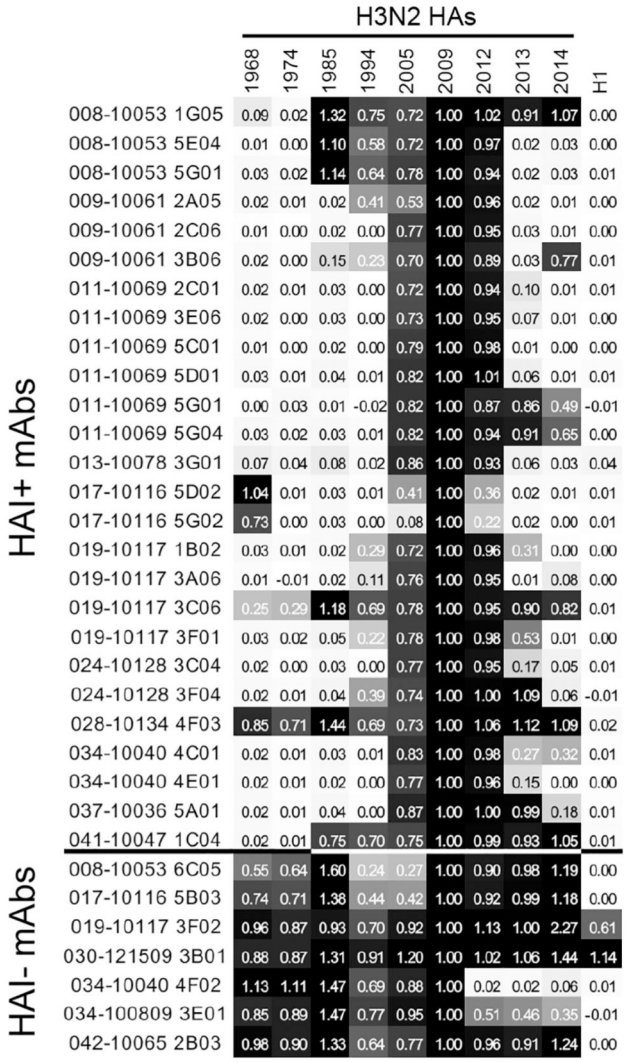

Figure 3. Binding of mAbs to Historical H3N2 Strains

ELISAs were completed with each mAb and a panel of historical H3N2 strains and the A/California/07/2009 H1N1 strain. Colors of each square range from white (0% of binding to WT) to black (100% of binding to WT). Binding values are the average of three independent experiments, while the value in each square indicates the fraction of binding relative to the A/Victoria/210/2009 vaccine strain. H3N2 strain information is reported in the Key Resources Table.

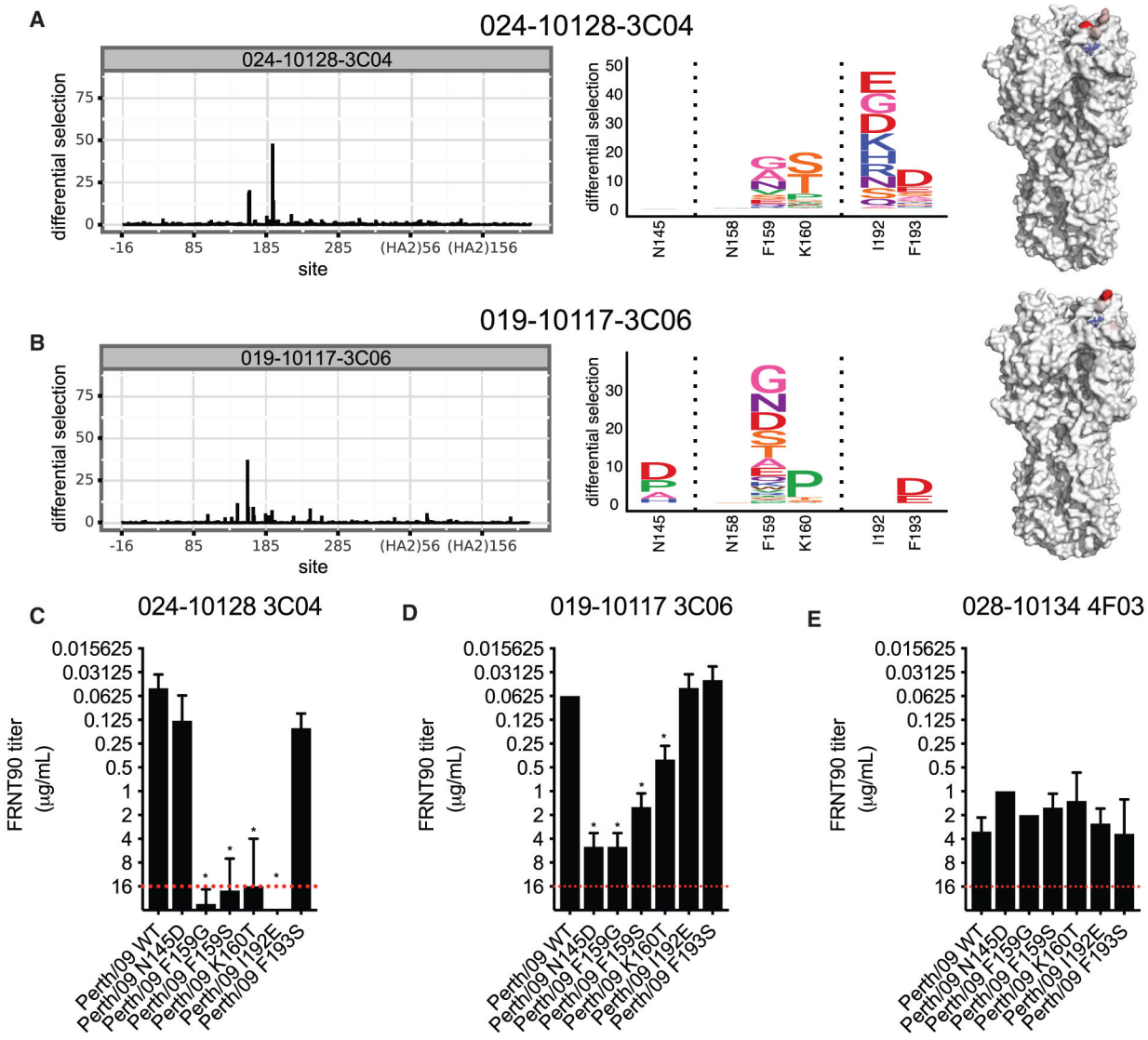

Figure 4. Mutational Antigenic Profiling of mAbs Targeting Antigenic Site B and the RBS

Deep mutational scanning experiments were completed to identify resistant viral fractions that survived after mAb selection.

(A and B) Logo plots showing the selection of amino acid substitutions and locations of these substitutions on the HA structure after selection with the 024-10128-3C04 mAb (A) and the 019-10117-3C06 mAb (B).

(C–E) Neutralization assays were completed with viruses that had several of the substitutions identified in deep mutational scanning experiments. Each panel shows neutralization of a single mAb against WT virus and viral mutants identified by mutational antigenic profiling. A red dashed line indicates the limit of detection (each mAb was tested at a starting concentration of 16 μg/mL). Neutralization titers shown are the geometric mean, and error bars denote the geometric SD of three independent experiments. Statistical analyses of differences between neutralization (FRNT) titers against WT and mutant viruses

were done using a one-way ANOVA with Dunnett's test for multiple comparisons. *$p < 0.05$.

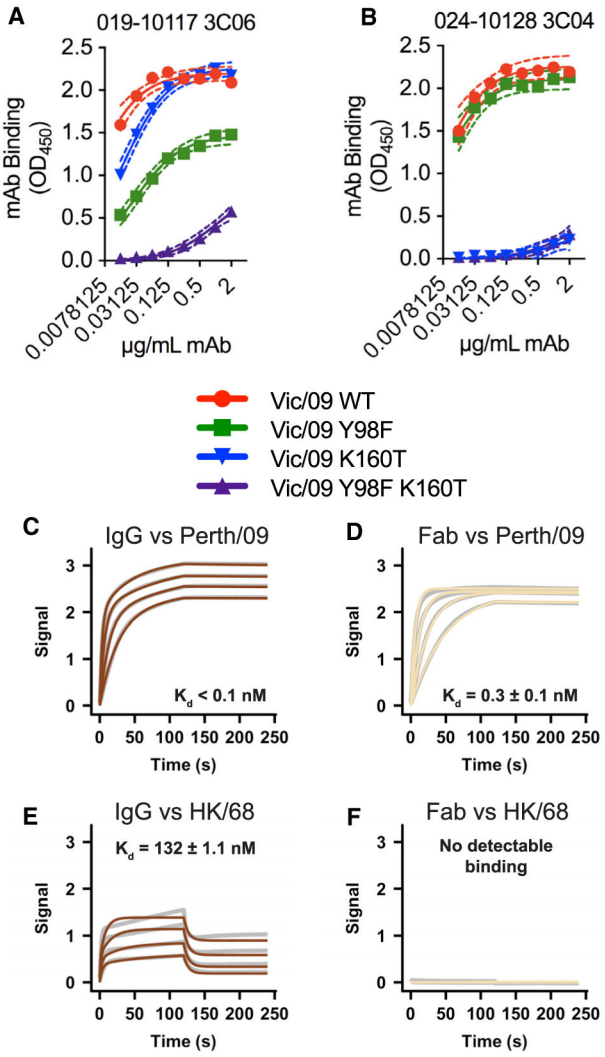

Figure 5. mAb 019-10117 3C06 Requires RBS Contacts and Bivalent Binding for Cross-Reactivity

(A and B) ELISAs were completed using the 019-10117-3C06 mAb (A) and the 024-10128-3C04 mAb (B) and plates coated with mammalian-expressed recombinant A/Victoria/210/2009 (Vic/09) HA VLPs with only Y98F, only K160T, or Y98F and K160T. ELISA binding curves from experimental triplicates are shown with one site—specific binding curves fit to the data (GraphPad Prism). (C–F) Dashed lines represent the 95% confidence interval (CI) for each curve fit. Biolayer interferometry (BLI) was used to measure binding of 019-10117-3C06 IgG and Fab to A/Perth/16/2009 (Perth/09) (C and D) and A/Hong Kong/1/1968 (HK/68) (E and F) baculovirus-expressed recombinant HA proteins. Gray lines represent the response curve and colored lines represent the 1:1 binding model (for Fab) or heterogenous ligand model (for IgG).

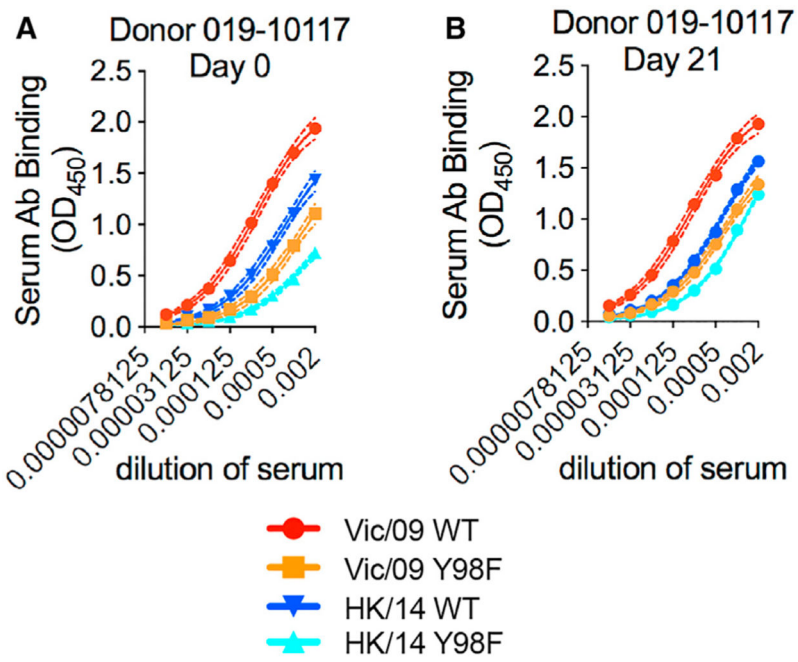

Figure 6. Rare Individuals Have High Levels of RBS-Targeting Antibodies in Serum

ELISAs were completed with serum from Donor 019-10117 with plates coated with mammalian-expressed recombinant A/Victoria/210/2009-WT HA (Vic/09 WT), A/Hong Kong/4801/2014-WT HA (HK/14 WT), and Y98F HA RBS mutants of both strains (Vic/09 Y98F, HK/14 Y98F).

(A and B) ELISAs were completed with serum collected before vaccination (day 0) (A) or 21 days after vaccination (B). Serum antibodies collected pre- and post-vaccination from 019-10117 exhibited reduced binding to A/Victoria/210/2009 HA with the Y98F substitution and the A/Hong Kong/4801/2014 HA with the Y98F substitution. Dashed lines represent the 95% CI for each site, specific binding curve fit. Data shown are from three independent experiments.

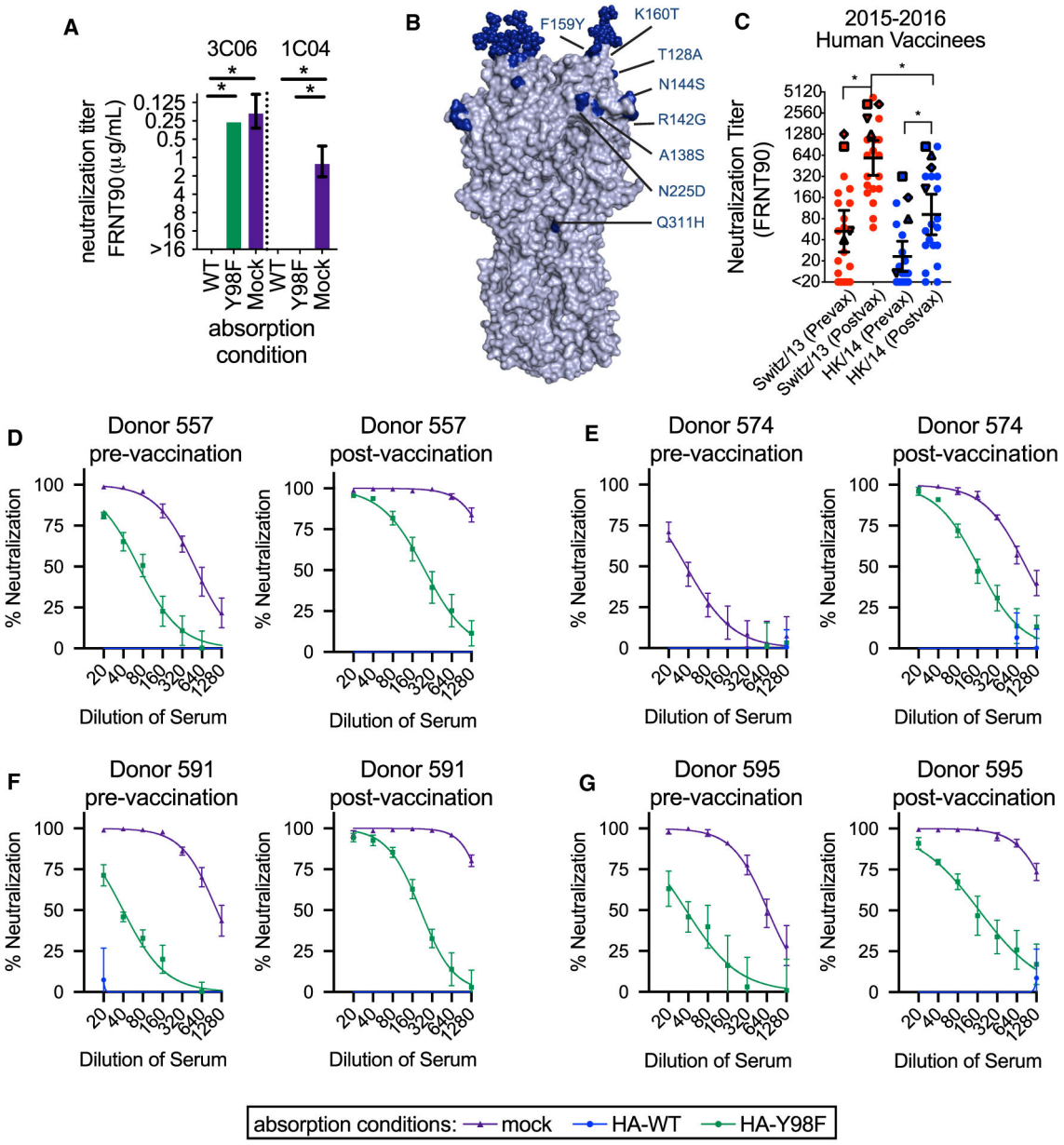

Figure 7. RBS Antibodies Contribute to Neutralizing Titers against an Antigenically Mismatched Strain

(A) Absorption assays were completed with the 019-10117-3C06 (abbreviated 3C06) and 041-10047-1C04 (abbreviated 1C04) mAbs. The A/Hong Kong/4801/2014-WT HA depleted both mAbs, while absorption with A/Hong Kong/4801/2014-Y98F HA did not deplete the 019-10117 3C06 mAb. Titers shown are the geometric mean of three independent experiments, and error bars show the geometric SD. Statistical comparisons between WT and the Y98F and mock absorption conditions were done using a one-way ANOVA with Dunnett's test for multiple comparisons. *$p<0.05$.

(B) Residue differences between the HA of the 2015–2016 vaccine strain (A/Switzerland/9715293/2013) and circulating strain (A/Hong Kong/4801/2014) are shown in dark blue on the H3 structure.

(C) Neutralization assays were completed with serum collected pre- and post-vaccination from individuals receiving the 2015–2016 seasonal influenza vaccine. Assays were completed with the vaccine strain (A/Switzerland/9715293/2013) and circulating strain (A/Hong Kong/4801/2014). Titers shown are the geometric mean of three independent experiments. Black lines indicate geometric mean and geometric 95% CI for each group, and statistical comparisons were made using the nonparametric Friedman test with correction for multiple comparisons. Statistically significant differences between groups are noted (*$p < 0.05$). Neutralization titers for select individuals are noted with symbols: (557: upward-pointing triangle, 574: downward-pointing triangle, 591: square, 595: diamond). (D–G) Absorption assays were completed with serum from individuals pre- and post-vaccination and neutralization of the A/Hong Kong/4801-WT virus was measured using an FRNT assay. Each separate panel shows pre- and post-vaccination neutralization titers for a single individual. Sera were absorbed with 293F cells expressing A/Hong Kong/4801-WT HA (WT), A/Hong Kong/4801 HA with a Y98F substitution (Y98F), or no HA (mock). Neutralization curves from at least three independent absorption experiments are shown, with error bars for individual data points showing the SEM.

KEY RESOURCES TABLE

REAGENT or RESOURCE	SOURCE	IDENTIFIER
Antibodies		
Peroxidase-Conjugated Goat Affinity Purified Antibody to Mouse IgG (Whole Molecule)	MP Biomedical	Cat# 0855563
Peroxidase AffiniPure F(ab')$_2$ Fragment Goat Anti-Human IgG	Jackson ImmunoResearch Laboratories	Cat# 109-036-098
Mouse anti-NP antibody (IC5-1B7)	BEI Resources	Cat# NR-43899
Monoclonal Anti-Human Influenza A (H3N2) (Clone F49)	Takara Bio	Cat# M146
Monoclonal Anti-Human Influenza A (H1N1, H2N2) (Clone C179)	Takara Bio	Cat# M145
008-10053 1G05	This study	N/A
008-10053 5E04	This study	N/A
008-10053 5G01	This study	N/A
008-10053 6C05	This study	N/A
009-10061 2A05	This study	N/A
009-10061 2C06	This study	N/A
009-10061 3B06	This study	N/A
011-10069 2C01	This study	N/A
011-10069 3E06	This study	N/A
011-10069 5C01	This study	N/A
011-10069 5D01	This study	N/A
011-10069 5G01	This study	N/A
011-10069 5G04	This study	N/A
013-10078 3G01	This study	N/A
017-10116 5B03	This study	N/A
017-10116 5D02	This study	N/A
017-10116 5G02	This study	N/A
019-10117 1B02	This study	N/A
019-10117 3A06	This study	N/A
019-10117 3C06	This study	N/A
019-10117 3F01	This study	N/A
019-10117 3F02	This study	N/A
024-10128 3C04	This study	N/A
024-10128 3F04	This study	N/A
028-10134 4F03	This study	N/A
030-121509 3B01	This study	N/A
034-10040 4C01	This study	N/A
034-10040 4E01	This study	N/A
034-10040 4F02	This study	N/A
034-100809 3E01	This study	N/A
037-10036 5A01	This study	N/A
041-10047 1C04	This study	N/A

REAGENT or RESOURCE	SOURCE	IDENTIFIER
042-10065 2B03	This study	N/A
Bacterial and Virus Strains		
A/Hong Kong/1/1968 H3N2	BEI	NR-346
A/Scotland/840/1974 H3N2	BEI	NR-3662
A/Mississippi/1/1985 H3N2	BEI	NR-3502
A/Johannesburg/33/1994 H3N2	BEI	NR-3656
A/Wisconsin/67/2005 H3N2	IRR	FR-397
A/Victoria/210/2009 H3N2 (X-187, GenBank HQ378745) and point mutants	Reverse-genetics derived, this study	N/A
A/Perth/16/2009 H3N2 and point mutants	Reverse-genetics derived, this study and (Lee et al., 2018)	N/A
A/Texas/50/2012 H3N2	Reverse-genetics derived, (Chambers et al., 2015)	N/A
A/Switzerland/9715293/2013 H3N2 (GISAID EPI543062)	Reverse-genetics derived	N/A
A/Hong Kong/4801/2014 H3N2 (GenBank KT838266.1)	Reverse-genetics derived, this study	N/A
A/California/07/2009 H1N1 (GenBank NC_026433.1) with D225G substitution	Reverse-genetics derived, this study	N/A
A/Perth/16/2009 mutational library	(Lee et al., 2018)	N/A
Biological Samples		
Human serum samples before and after 2010-2011 vaccination	This study	N/A
Human serum samples before and after 2015-2016 vaccination	This study	N/A
Chemicals, Peptides, and Recombinant Proteins		
TrueBlue TMB Peroxidase Substrate	KPL-Seracare	Cat# 5510-0030
SureBlue TMB Peroxidase Substrate	KPL-Seracare	Cat# 5120-0077
Modified Eagle Medium (MEM)	Corning Cellgro	Cat# MT10-010-CM
Dulbecco's Modified Eagle Medium (DMEM)	Corning Cellgro	Cat# MT10-013-CM
FreeStyle 293 Expression Medium	Thermo Fisher	Cat# 12338026
Fetal Bovine Serum	Sigma-Aldrich	Cat# F0926-100ML
HEPES buffer	Thermo Fisher	Cat# 25-060-CI
Gentamicin	Thermo Fisher	Cat# 15750060
Trypsin, TPCK Treated	Thermo Fisher	Cat# 20233
Bovine Serum Albumin	Sigma-Aldrich	Cat# A8022-500G
Hydrochloric acid 37%	Sigma-Aldrich	Cat# 258148-500ML
Receptor-destroying enzyme II	VWR	Cat# 10753-482
Tween 20	Thermo Fisher	Cat# 9005-64-5
Methyl cellulose	Sigma-Aldrich	Cat# M0512
Paraformaldehyde 32% solution	Electron Microscopy Sciences	Cat# 15714-S
Triton X-100	Sigma-Aldrich	Cat# 10789704001
Fat-free milk, dry powder	Dot Scientific, Inc	Cat# DSM17200-1000
293fectin Transfection Reagent	Thermo Fisher	Cat# 12347019
Ni-NTA Agarose	QIAGEN	Cat# 30210
A/Hong Kong/1/1968 recombinant HA	This study, from baculovirus	N/A
A/Perth/16/2009 recombinant HA	This study, from baculovirus	N/A

REAGENT or RESOURCE	SOURCE	IDENTIFIER
A/Victoria/210/2009 WT recombinant HA	This study, from 293F mammalian expression	N/A
A/Victoria/210/2009 Y98F recombinant HA	This study, from 293F mammalian expression	N/A
A/Hong Kong/4801/2014 WT recombinant HA	This study, from 293F mammalian expression	N/A
A/Hong Kong/4801/2014 Y98F recombinant HA	This study, from 293F mammalian expression	N/A
Millipore Protein A/G Magnetic beads	EMD Millipore	Cat # LSKMAGAG10
Critical Commercial Assays		
Quikchange II XL Mutagenesis Kit	Agilent Technologies	Cat# 200522
Deposited Data		
HA mutant libraries selected by monoclonal antibodies	This paper	SAMN10183083
HA monoclonal antibody selection controls	This paper	SAMN10183146
Human Ig-V_H and IgV_L sequences	GenBank	MH205211, MH205413, KM603994, and MN483379-MN483441
Experimental Models: Cell Lines		
Freestyle 293F	Thermo Fisher	Cat# R79007
293T	NIH	N/A
MDCK	NIH	N/A
MDCK-SIAT1	NIH	N/A
Recombinant DNA		
Plasmid: HIV gag (pTR994)	University of Georgia	N/A
Plasmid: A/Puerto Rico/1934 NA (VRC9776)	NIH	N/A
Plasmid: HAT protease (HAT in pCAGGS)	Doms lab, Penn	N/A
Plasmid: influenza reverse genetics plasmids	NIH	N/A
Plasmid: A/Victoria/210/2009 HA WT X-187 (GenBank HQ378745) and point mutants (for VLP production)	This study	N/A
Plasmid: A/Hong Kong/4801/2014 HA WT (GenBank KT838266.1) and point mutants (for absorption assays)	This study	N/A
008-10053 1G05_Vκ	This study	N/A
008-10053 5E04_Vκ	This study	N/A
008-10053 5G01_Vκ	This study	N/A
008-10053 6C05_Vκ	This study	N/A
009-10061 2A05_Vλ	This study	N/A
009-10061 2C06_Vλ	This study	N/A
009-10061 3B06_VK	This study	N/A
011-10069 2C01_Vλ	This study	N/A
011-10069 3E06_Vλ	This study	N/A
011-10069 5C01_Vλ	This study	N/A
011-10069 5D01_Vλ	This study	N/A
011-10069 5G01_Vλ	This study	N/A
011-10069 5G04_Vλ	This study	N/A
013-10078 3G01_Vλ	This study	N/A

REAGENT or RESOURCE	SOURCE	IDENTIFIER
017-10116 5B03_Vκ	This study	N/A
017-10116 5D02_Vκ	This study	N/A
017-10116 5G02_Vκ	This study	N/A
019-10117 1B02_Vκ	This study	N/A
019-10117 3A06_Vλ	This study	N/A
019-10117 3C06_Vλ	This study	N/A
019-10117 3F01_Vλ	This study	N/A
019-10117 3F02_Vλ	This study	N/A
024-10128 3C04_Vλ	This study	N/A
024-10128 3F04_Vλ	This study	N/A
028-10134 4F03_Vκ	This study	N/A
030-121509 3B01_Vκ	This study	N/A
034-10040 4C01_Vκ	This study	N/A
034-10040 4E01_Vλ	This study	N/A
034-10040 4F02_Vκ	This study	N/A
034-100809 3E01_Vκ	This study	N/A
037-10036 5A01_Vλ	This study	N/A
041-10047 1C04_Vλ	This study	N/A
042-10065 2B03_Vλ	This study	N/A
008-10053 1G05_IgG1	This study	N/A
008-10053 5E04_IgG1	This study	N/A
008-10053 5G01_IgG1	This study	N/A
008-10053 6C05_IgG1	This study	N/A
009-10061 2A05_IgG1	This study	N/A
009-10061 2C06_IgG1	This study	N/A
009-10061 3B06_IgG1	This study	N/A
011-10069 2C01_IgG1	This study	N/A
011-10069 3E06_IgG1	This study	N/A
011-10069 5C01_IgG1	This study	N/A
011-10069 5D01_IgG1	This study	N/A
011-10069 5G01_IgG1	This study	N/A
011-10069 5G04_IgG1	This study	N/A
013-10078 3G01_IgG1	This study	N/A
017-10116 5B03_IgG1	This study	N/A
017-10116 5D02_IgG1	This study	N/A
017-10116 5G02_IgG1	This study	N/A
019-10117 1B02_IgG1	This study	N/A
019-10117 3A06_IgG1	This study	N/A
019-10117 3C06_IgG1	This study	N/A
019-10117 3F01_IgG1	This study	N/A
019-10117 3F02_IgG1	This study	N/A
024-10128 3C04_IgG1	This study	N/A

REAGENT or RESOURCE	SOURCE	IDENTIFIER
024-10128 3F04_IgG1	This study	N/A
028-10134 4F03_IgG1	This study	N/A
030-121509 3B01_IgG1	This study	N/A
034-10040 4C01_IgG1	This study	N/A
034-10040 4E01_IgG1	This study	N/A
034-10040 4F02_IgG1	This study	N/A
034-100809 3E01_IgG1	This study	N/A
037-10036 5A01_IgG1	This study	N/A
041-10047 1C04_IgG1	This study	N/A
042-10065 2B03_IgG1	This study	N/A
Software and Algorithms		
GraphPad Prism 7.0	GraphPad Software, Inc.	https://graphpad.com
PyMOL	Schrödinger	https://pymol.org
Other		
Turkey whole blood in ACD	Lampire Biological Laboratories	7209401
Octet Red Biolayer instrument	ForteBio	N/A
Streptavidin (SA) Biosensors	ForteBio	#18-5019
Immunospot ELISpot Imager	Cellular Technology Limited	N/A